DE GRUYTER

Chemical Papers 69 (4) 527–535 (2015)
DOI: 10.1515/chempap-2015-0061

ORIGINAL PAPER

A simple pyridine-based colorimetric chemosensor for highly sensitive and selective mercury(II) detection with the naked eye

[a]Jian-Ting Pan, [a]Fei Zhu, [a]Lin Kong, [a]Long-Mei Yang, [b]Xu-Tang Tao, [a]Yu-Peng Tian, [c]Hong-Bo Lu, [a,b,c]Jia-Xiang Yang*

[a]*Department of Chemistry, Key Laboratory of Functional Inorganic Materials of Anhui Province, Anhui University, Hefei 230039, China*

[b]*State Key Laboratory Materials, Shandong University, Jinan 502100, China*

[c]*Academy of Opto-Electronic Technology, Hefei University of Technology, Hefei 230026, China*

Received 4 June 2014; Revised 17 August 2014; Accepted 17 September 2014

Two easily-prepared pyridine-based derivatives of (*Z*)-2-(4-amino-phenyl)-3-(pyridine-4-yl)acrylonitrile (*I*) and (*Z*)-2-phenyl-3-(pyridin-4-yl)acrylonitrile (*II*) were designed, synthesised and characterised. Due to the formation of a complex with Hg^{2+}, hence leading to an enhanced ICT effect, *I* exhibits a visible colour change from light yellow to orange, rendering it suitable for use as a naked-eye sensor for rapid detection of Hg^{2+} in an aqueous ethanol solution. When mixed with Hg^{2+}, *I* interacts with Hg^{2+} in a 2 : 1 (Y1–Hg^{2+}) stoichiometry via a coordination bond with an association constant of 7.7×10^8 M^{-2} ($R^2 = 0.96$). The present probe *I* exhibits excellent reproducibility, reversibility, sensitivity and selectivity with the presence of low concentration of Hg^{2+} (1.74×10^{-10} M).
© 2014 Institute of Chemistry, Slovak Academy of Sciences

Keywords: mercury ion sensor, pyridine, colorimetric, specific selectivity, easy-to-prepare, charge transfer

Introduction

Contamination by heavy metal ions, in particular the mercury ion (Hg^{2+}), has caused serious harm to the environment and human health. Hg^{2+} can easily penetrate biological membranes and cause serious damage to the brain, central nervous system and kidneys, in addition to the respiratory system, skin, blood and eyes. (Azevedo-Pereira & Soares, 2010; Gundacker et al., 2010; Hansen et al., 2011; Chemnasiri & Hernandez, 2012; Farhadi et al., 2012; Jenssen et al., 2012; Koenig et al., 2013; Xing et al., 2013; Zhao et al., 2014; Zhong et al., 2014). Hence, it is imperative to screen suitable Hg^{2+} detection systems with high selectivity, sensitivity and reliability. Many methods have been developed specifically for Hg^{2+} ion detection (Coronado et al., 2005; Kim et al., 2010, 2012; Misra & Shahid, 2010; Cheng et al., 2011; Dalapati et al., 2011; Tian & Ihmels, 2011; Ren et al., 2012; Chen et al., 2013; Goswami et al., 2013; Lu et al., 2013; Madhu et al., 2013; Shafeekh et al., 2013; Bera et al., 2014; Carter et al., 2014; Huang et al., 2014; Li et al., 2014; Thirupathi et al., 2014). For example, Thirupathi et al. (2014) reported a ratiometric fluorescence chemosensor based on tyrosine derivatives for monitoring mercury ions in aqueous solutions. Li et al. (2014) reported cyclometallated ruthenium complex-modified upconversion nanophosphorous derivatives for the selective detection of Hg^{2+} ions in water to improve the selectivity and sensitivity of a measurement, by using ratiometric measurements. The ratiometric method can overcome the limitations of intensity measurements due to a built-in correction for environmental effects, and makes possible signal-rationing, thereby increasing the dynamic range. The perceived colour change would be useful not only for the ra-

*Corresponding author, e-mail: jxyang@ahu.edu.cn

Brought to you by | New York University Bobst Library Technical Services
Authenticated
Download Date | 5/27/15 5:46 PM

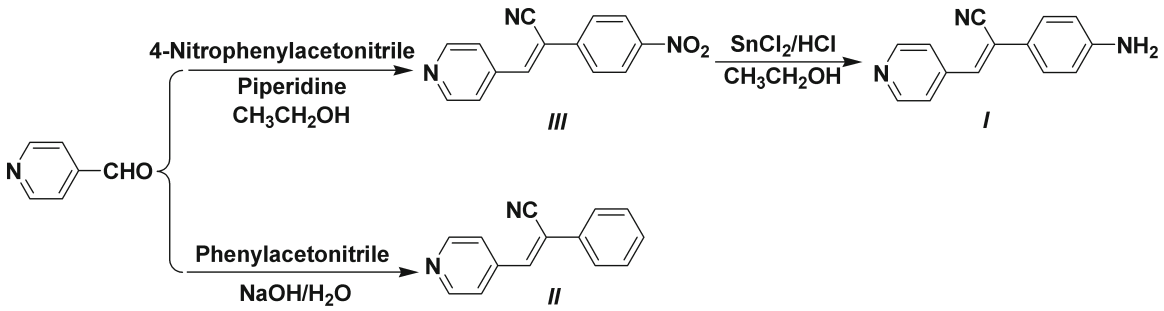

Fig. 1. Synthetic routes for *I* and *II*.

tiometric method of detection but also for rapid visual sensing. Although many fluorometric ratiometric probes for Hg^{2+} have been developed (Aït-Haddou et al., 2001; Chen & Chen, 2005; Gunnlaugsson et al., 2005; Liang et al., 2007; Guo et al., 2010; Hu & Chen, 2011; Wen et al., 2011), the number of selective and sensitive colorimetric sensors based on the mechanism of internal charge transfer (ICT) available for the detection of Hg^{2+} ions in aqueous media remains limited (Sheng et al., 2008; Mei et al., 2012; Shellaiah et al., 2013; Wang et al., 2013). Moreover, many existing colorimetric probes for Hg^{2+} are subject to some disadvantages such as complicated synthetic routes, low sensitivity, high cost and lengthy response time. Accordingly, there remains a need for new simple and easily-prepared colorimetric probes in an aqueous medium for the rapid, sensitive, selective visual detection of Hg^{2+} over other relevant metal ions (Lee et al., 2007).

The current study details the synthesis of two simple structural compounds *I* and *II* (Fig. 1) and the photochemical elucidation of their selective colour changes in the presence of Hg^{2+} ions and the possible signalling mechanism. *I* is a donor-π-acceptor (D-π-A)-type structural compound, in which the two functional groups aminophenyl and pyridine ring are connected through a double bond, with the amino group moiety acting as the electron donor and the pyridinyl group as the electron acceptor. The design of this compound seeks to make use of the coordination ability of the well-known pyridine structure unit and the strong electron-donating ability and hydrophilic characteristic of the amine group which can act not only as a signal group but also enhance the water solubility. Probe *I* acts as a naked-eye sensor for the Hg^{2+} ion with high selectivity and sensitivity as well as good reversibility in an aqueous ethanol solution, accompanied by a colour change from light yellow to orange due to its ICT increase. In order to elucidate the role of the signal group to the colorimetric-sensing abilities for Hg^{2+}, compound *II* which was without the amino-group was also synthesised. This study highlights a new concept and design of a sensor using a simple synthetic method, avoiding complicated structures and varied detection methods.

Experimental

All commercially available chemicals were of reagent grade and used without further purification. Prior to use, all solvents were purified using the conventional methods. All of the starting materials are readily available at low cost. The metal salts tested included $Hg(ClO_4)_2 \cdot 3H_2O$, $CuSO_4 \cdot 5H_2O$, $CdSO_4 \cdot 8H_2O$, $MnSO_4 \cdot H_2O$, $ZnSO_4 \cdot 7H_2O$, $MgSO_4$, K_2SO_4, $AgNO_3$, $Pb(NO_3)_2$, $CoCl_2 \cdot 6H_2O$, $NiCl_2 \cdot 6H_2O$, $CaCl_2$ and $BaCl_2 \cdot 2H_2O$ purchased from Aldrich (USA) and used as received.

^{1}H NMR and ^{13}C NMR spectra were recorded on a Bruker Avance 400 MHz NMR spectrometer (Bruker, Switzerland) at ambient temperature using DMSO-d_6 as solvent; chemical shifts are given in ppm (δ) values (internal standards TMS for ^{1}H and ^{13}C NMR spectra). The splitting patterns were described as singlet (s), doublet (d), triplet (t), quartet (q) or multiplet (m). Elemental analysis was recorded on a Vario ELIII. The high-resolution mass spectra (HR-MS) were recorded on a Thermo Fisher LTQ-Orbitrap XL mass spectrometer (Thermo Fisher, USA) using an electrospray ion source (ESI).The FT-IR spectra were recorded using a Nicolet 380 FT-IR spectrometer instrument (KBr discs) in the range of 400–4000 cm^{-1} (Thermo Fisher, USA). The UV-VIS absorption spectra were recorded on the UV-265 spectrophotometer (Shimadzu, Japan) with a quartz cuvette (path length of 1 cm) and studies were performed in AR grade ethanol and distilled water. The one-photon excited fluorescence (OPEF) spectra measurements were performed using the Hitachi F-7000 fluorescence spectrophotometer (Tianmei,China).

(*Z*)-2-(4-Nitrophenyl)-3-(pyridin-4-yl)acrylonitrile (*III*): a mixture of 4-pyridinecarboxaldehyde (0.214 g, 2 mmol) and 4-nitrophenylacetonitrile (0.324 g, 2 mmol) in 20 mL of ethanol were refluxed for approximately 1 h after adding piperidine drop-wise. The resulting precipitate was cooled to ambient temperature, washed with ethanol and recrystallised from ethanol to afford *III* as a white solid (0.452 g, 90 % yield). FT-IR (KBr, cm^{-1}) selected bands: 3108 (w), 3071 (w), 3041 (w), 2220 (m), 1597 (s), 1514 (s), 1344 (s), 856 (s). ^{1}H NMR (DMSO-d_6, 400 MHz) δ: 7.85 (d, $J = 6.0$

Brought to you by | New York University Bobst Library Technical Services
Authenticated
Download Date | 5/27/15 5:46 PM

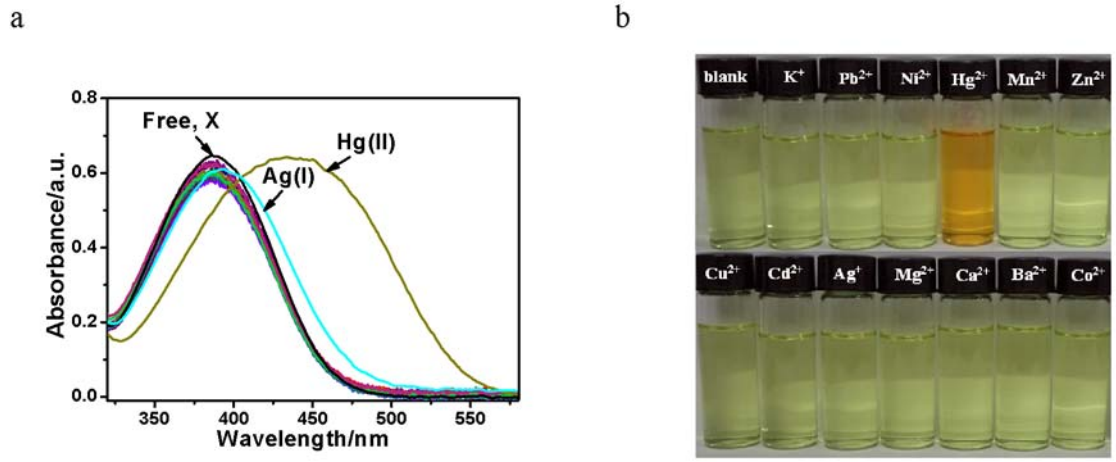

Fig. 2. UV-VIS spectra of *I* (50.0 μM) on addition of metal ions: K^+, Pb^{2+}, Ni^{2+}, Hg^{2+}, Mn^{2+}, Zn^{2+}, Cu^{2+}, Cd^{2+}, Ag^+, Mg^{2+}, Ca^{2+}, Ba^{2+} and Co^{2+} (5.0 eq.) in ethanol : H_2O (9 : 1, vol.) solvent (a). Naked-eye image of *I*–M complexes (b).

Hz, 2H), 8.09 (d, J = 8.8 Hz, 2H), 8.35 (s, 1H), 8.39 (d, J = 8.8 Hz, 2H), 8.81 (m, J = 6.0 Hz, 2H). ^{13}C NMR (DMSO-d_6, 100 MHz) δ: 112.93, 116.37, 122.72, 124.32, 127.47, 139.01, 140.19, 143.86, 147.85, 150.54.

(*Z*)-2-(4-Aminophenyl)-3-(pyridine-4-yl)acrylonitrile (*I*): a mixture of compound *III* (0.251 g, 1 mmol) and $SnCl_2$ (0.949 g, 5 mmol) in 20 mL of ethanol were stirred at 80 °C for 2 h. The resulting solution was cooled to ambient temperature and the pH adjusted to 8, then extracted with a large amount of ethyl acetate and the volatiles removed under vacuum. The residue was purified by flash silica gel chromatography (ethyl acetate : petroleum ether = 1 : 5 vol.) to afford *I* as an orange-red solid (0.166 g, 75 % yield). FT-IR (KBr, cm^{-1}) selected bands: 3390 (m), 3317 (m), 3032 (w), 2923 (w), 2849 (w), 2214 (m), 1584 (s), 1515 (s), 1415 (s), 832 (s). ^{1}H NMR (DMSO-d_6, 400 MHz) δ: 5.79 (s, 2H), 6.66 (d, J = 8.8 Hz, 2H), 7.49 (d, J = 8.4 Hz, 2H), 7.70 (s, 1H), 7.73 (d, J = 6.0 Hz, 2H), 8.68 (d, J = 6.4 Hz, 2H). ^{13}C NMR (DMSO-d_6, 100 MHz) δ: 113.78, 115.01, 117.43, 119.79, 122.27, 127.34, 132.90, 141.50, 150.23, 150.95. HR-MS (ESI-MS): m/z = 222.1021 ([M + H]$^+$), calc. for $[C_{14}H_{12}N_3]^+$ = 222.1031.

(*Z*)-2-Phenyl-3-(pyridin-4-yl)acrylonitrile (*II*): a mixture of 4-pyridinecarboxaldehyde (0.550 g, 5 mmol) and phenylacetonitrile (0.585 g, 5 mmol) in 30 mL of H_2O, 6 mL of 5 mass % aqueous NaOH solution was added drop-wise. The mixture was stirred at ambient temperature for 12 h to afford a white precipitate. The precipitate was filtered, washed with water and dried to afford *II* as a white solid (0.978 g, 94 % yield). FT-IR (KBr, cm^{-1}) selected bands: 3061 (w), 3033 (w), 2927 (w), 2214 (m), 1590 (s), 1543 (s), 1498 (s), 758 (s), 683 (s). ^{1}H NMR (DMSO-d_6, 400 MHz) δ: 7.50–7.58 (m, 3H), 7.82 (d, J = 6.4 Hz, 4H), 8.11 (s, 1H), 8.77 (d, J = 5.6 Hz, 2H). ^{13}C NMR (DMSO-d_6, 100 MHz) δ: 114.70, 116.97, 122.62, 126.13, 129.27, 130.07, 132.93, 140.20, 140.74, 150.43. HR-MS (ESI-MS): m/z = 207.0918 ([M+H]$^+$), calc. for $[C_{14}H_{11}N_2]^+$ = 207.0922.

Results and discussion

I and *II* were synthesised by simple procedures and characterised by ^{1}H and ^{13}C NMR, FT-IR and MS. The original spectra are available in Supplementary Information.

The chromophore of chemosensor *I* was based on a D-π-A system, which could exhibit an obvious colour change, thereby making the chemosensor colorimetric. The selective and sensitive signal response of *I* to Hg^{2+} ions was embodied in absorption. All titration experiments were carried out in ethanol : H_2O (9 : 1, vol.) as a solvent.

Fig. 2 shows that K^+, Pb^{2+}, Ni^{2+}, Mn^{2+}, Zn^{2+}, Cu^{2+}, Cd^{2+}, Mg^{2+}, Ca^{2+}, Ba^{2+} and Co^{2+} ions do not cause any significant change in the *I* spectrum; only Ag^+ ions result in a 9 nm red-shift, which could probably be attributed to their low affinity to the receptor *I*. However, the effect of Ag^+ ions is negligible compared with the marked change in the UV-VIS spectrum after adding Hg^{2+}. The absorption spectrum changes a little after the combination with different metal ions, demonstrating that the receptor *I* possesses specific colorimetric selectivity to Hg^{2+} in ethanol : H_2O (9 : 1, vol.) binary solutions. Spectral data were recorded at 1 min after adding Hg^{2+} ions, there was a marked change in the absorption spectra of compound *I*, with a new band appearing at 437 nm. The image clearly shows, a colour change after adding mercury ion to the solution which is significantly different from others, changing from light yellow to orange, suggesting that chemosensor *I* can serve as a "naked-eye" indicator of Hg^{2+} ions. Moreover, the wavelength of maximum excitation peak also red-shifts from 384 nm to 437 nm. This result demonstrates the unique selectivity of *I* towards Hg^{2+}. Hence, it may be predicted that

Brought to you by | New York University Bobst Library Technical Services
Authenticated
Download Date | 5/27/15 5:46 PM

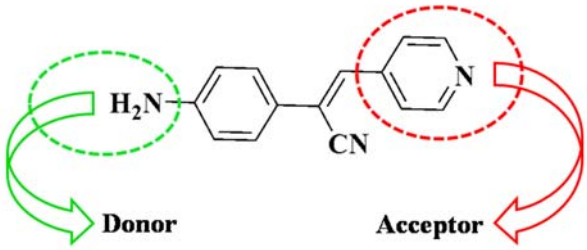

Fig. 3. Representation of donor and acceptor part of receptor *I*.

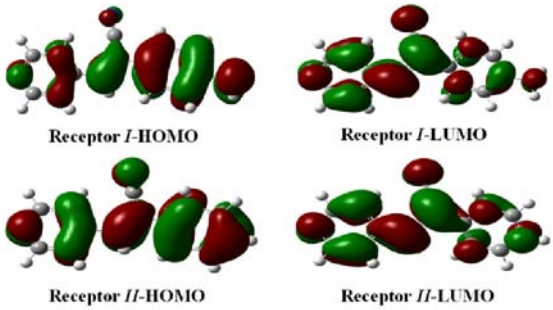

Fig. 4. HOMO and LUMO orbital of receptors *I* and *II* calculated by B3LYP method with the 6-31G* basis-set.

the addition of the Hg^{2+} ions increases the ICT effect. The colorimetric sensor *I* is a conjugated form of two subunits: the aminophenyl and pyridine ring and the existing ICT (internal charge transfer) itself. When *I* bonded with Hg^{2+}, to some extent, most of the electron contributed to Hg^{2+}, which is responsible for the red shift of the UV-VIS spectra.

The design of receptor *I* makes it a fitting candidate to serve as an ICT probe. The pyridine ring is presumed to act as the electron acceptor while the remaining amine group is presumed to act as the donor (Fig. 3). The result of receptor *I* as an effective ICT probe was represented in terms of the major change in the absorption pattern as well as the visual appearance (from light yellow to orange) of the receptor *I* upon addition of Hg^{2+}. The receptor *II* was weakened by the missing NH_2 group. In order to state the importance of the role of amino groups in the donor in the colour change, compound *II* was tested under the same conditions. It does not exhibit any spectral changes upon the addition of metal ions (Fig. S1), showing that the amino groups act as a single group, and plays a vital role in the colour changes induced in the mercury, which can be observed by the naked eye.

The above design principles of receptors *I* and *II* were further elucidated by density functional theory (DFT) calculations carried out with the Gaussian 09 program. The value of *I* absorption peak was calculated at 380 nm and that of *II* at 300 nm; both were in good agreement with the experimental values of 384 nm and 304 nm, respectively, within an error range of 4 nm. The HOMO–LUMO orbitals of the energy-minimised structures of receptors *I* and *II* are shown in Fig. 4. Due to the existence of NH_2, *I* exhibited a better ICT than *II*, rendering it a better ICT probe.

To evaluate the sensing behaviour of *I* towards Hg^{2+}, the absorption spectral titration of *I* with Hg^{2+} in ethanol : H_2O (9 : 1, vol.) was carried out. Fig. 5 shows the changes in the absorption spectrum of *I* as a function of Hg^{2+} concentration at ambient temperature. In the absence of Hg^{2+} ions, the spectrum of probe *I* is characterised by an absorption band centred at 384 nm ($\varepsilon = 1.2 \times 10^4$ M^{-1} cm^{-1}). A new sharp absorption band at 437 nm appeared with the prior absorption band at 384 nm declining and absorbance increased with the increasing Hg^{2+} concentration (0–5.0 eq. of Hg^{2+}); when the Hg^{2+} concentration increased to 25.0 μM, the absorbance of *I* itself was slightly larger than of the new peak. On adding Hg^{2+} ions to the solution of *I*, the absorbance of the new peak did not change, due to the saturation effect. The limit of detection of the sensor *I* for Hg^{2+} was found to be 17.4 nM, using the equation for limit of detection $= 3\sigma/K$, where σ is the standard deviation of blank measurements and K is the slope between the absorbance and the Hg^{2+} concentration (Fig. S2) (Wei et al., 2013).

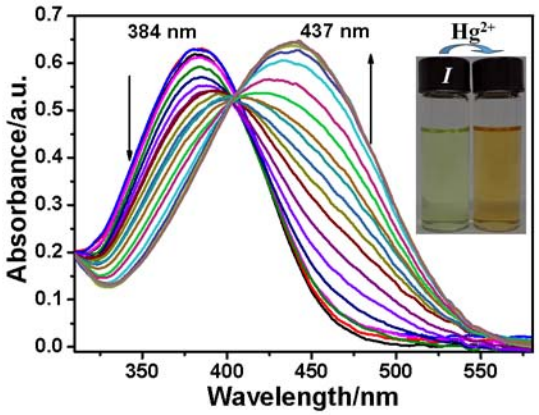

Fig. 5. UV-VIS titration spectra of *I* (50.0 μM) upon addition of various amounts of $Hg(ClO_4)_2$ (0–5.0 eq.; with step of 0.1 eq.) in ethanol : H_2O (9 : 1, vol.) solvent. Inset: colour change of *I*, *I* + Hg(II).

From the UV-VIS titration spectra, a definite ratiometry was noted, with one isosbestic point at 405 nm and a 2 : 1 reaction stoichiometry (*I* : Hg^{2+}), which shows that forming / indicates the formation of a new complex between the receptor *I* and Hg^{2+}; the formation of the new complex is responsible for generating the orange colour following the addition of $Hg(ClO_4)_2$ to the solution of the receptor *I* (Fig. 5). To corroborate the 2 : 1 ratio between *I* and Hg^{2+} ions, Job's plot analysis was also performed (Goswami et al., 2013). From the Job's plot, it can be observed

Brought to you by | New York University Bobst Library Technical Services
Authenticated
Download Date | 5/27/15 5:46 PM

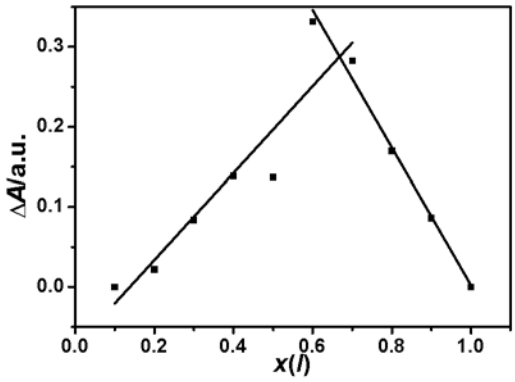

Fig. 6. Job's plot for 2 : 1 complexation of I with Hg(II) ion in ethanol : H_2O (9 : 1, vol.) solvent.

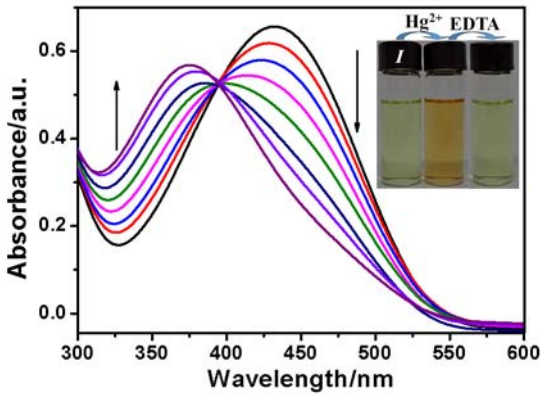

Fig. 7. UV-VIS titration spectra of I–Hg(II) complex upon EDTA addition in ethanol : H_2O (9 : 1, vol.) solvent. (Inset: colour change of I, I + Hg(II) and I + Hg(II) + EDTA).

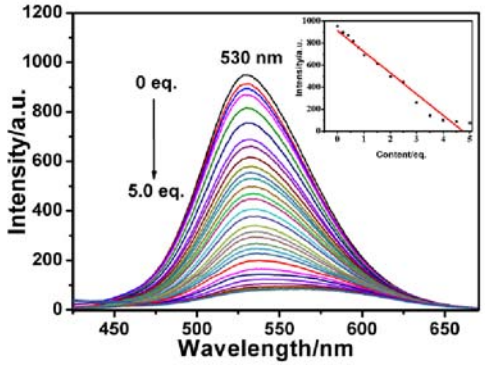

Fig. 8. Fluorescence emission spectra of I (50.0 μM) in ethanol : H_2O (9 : 1, vol.) solvent (λ_{ex} = 405 nm, Slit: 10 × 10) in the presence of increasing amount of $Hg(ClO_4)_2$ (0–5.0 eq.; with step of 0.1eq.) pre-dissolved in deionised water. (Inset: fluorescence intensity of solution of I containing different content of Hg^{2+} at λ_{em} = 530 nm).

that the absorbance variation measured ($\Delta A = A_{obs} - A_i$) achieved a maximum value at a molar fraction of ($x(I) = [I]/([I] + [Hg^{2+}])$) at approximately 0.64, confirming that a 2 : 1 stoichiometry was most probable for the binding mode of Hg^{2+} and I (Fig. 6). Based on the 2 : 1 stoichiometry, the association constant was determined by a non-linear least squares fit of data with the following equation (Fig. S3) as the reference method; the association constant of I for Hg^{2+} was calculated as 7.7×10^8 M^{-2} ($R^2 = 0.96$) (Yang et al., 2011).

In addition, the reversible research using ethylene diamine tetraacetic acid (EDTA) indicated the current response to be completely reversible (Fig. 7). It is of great interest that compound I could be regenerated by adding an excess of EDTA to the solution containing I–Hg^{2+}, then the mercury ions were captured by EDTA, as a result of the resurgence of I, which resulted in recovery of the original colour. This indicates the decomplexation of I–Hg^{2+}, as EDTA strips Hg^{2+} away from the binding side. EDTA forms a chelate with the mercury ion which is adequately stable. This stability results from the multiple sites within the ligand that give rise to a cage-like structure in which the Hg^{2+} is effectively surrounded and isolated from the solvent molecules (Chen et al., 2013; Shafeekh et al., 2013; Wang et al., 2013).

The fluorescence titration of I (50.0 μM) in the presence of different Hg^{2+} concentrations was also performed. Fig. 8 shows that sensor I exhibited a fluorescence emission at 530 nm. Upon increasing the concentration of Hg^{2+} to 25×10^{-5} M, the emission intensity at 530 nm gradually reduced, which can be explained by compound I itself having the intramolecular charge transfer process from amino group moiety to the pyridinyl group. When combined with Hg^{2+}, to some extent increasing the ICT effect, most of the electrons then contributed to the Hg^{2+}. (Zhu et al., 2008).

In order to understand the selectivity of I to Hg^{2+} ions, an interference study was carried out by the addition of different metal ions (5 eq.) to the solution of I in a particular order. As portrayed in Fig. 9, the detection of Hg^{2+} in the presence of other metal ions is not impeded, i.e., the interference in the detection of the Hg^{2+} is not observed. Hence, I can be used as a selective and sensitive colorimetric sensor for the Hg^{2+} ion by the naked eye.

The effect of pH influence on the UV-VIS response of I to Hg^{2+} was examined (Wu et al., 2010; Zhou et al., 2013). It is apparent from Fig. 10a that, over a pH range of 5–14, the visible absorption band centred at 354 nm was unchanged. A decrease in pH from 2 to 1 engendered a shift in the maximal absorption wavelength to 314 nm; this 40 nm shift was due to protonation of the pyridine ring and the amine groups to form the A-π-A structure. When the pH values were changed from 3 to 4, this engendered a shift in the maximal absorption wavelength to 403 nm; this 49 nm

Brought to you by | New York University Bobst Library Technical Services
Authenticated
Download Date | 5/27/15 5:46 PM

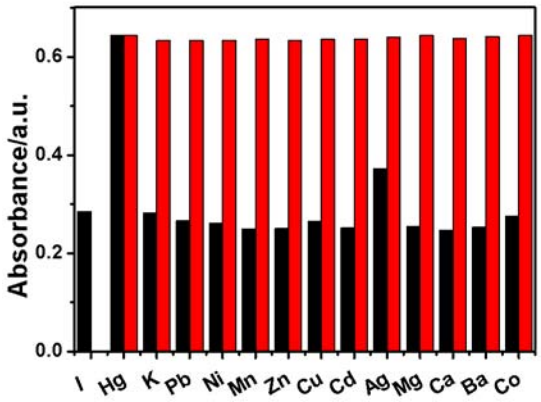

Fig. 9. Metal ion selectivity profile of receptor I (50.0 μM): change in absorbance intensity of receptor + 5.0 eq. M^{n+} (black bars); change in absorbance intensity of receptor + 5.0 eq. M^{n+}, followed by 5.0 eq. Hg^{2+} (red bars).

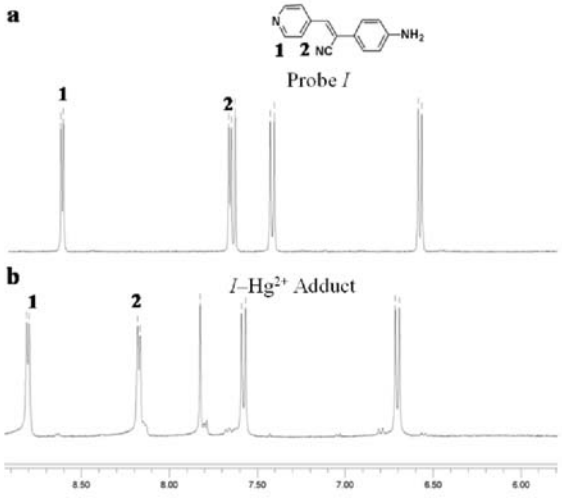

Fig. 11. Partial ^{1}H NMR spectra (400 MHz, DMSO-d_6) of probe I at 25 °C without metal cations (a) and in the presence of 0.5 eq. of Hg^{2+} (b).

shift was due to protonation of the pyridine ring only, thus enhancing the electron-withdrawing effect of the pyridine ring, inducing a red shift. This was further confirmed by adding Hg^{2+} (0–5.0 eq.) directly into the solutions of pH 1 and pH 4 (Figs. S4 and S5), with no obvious changes to each peak.

To gain an insight into the sensing mechanism and binding mode of I with Hg^{2+}, the FT-IR, MS, ^{1}H NMR and elemental analysis were investigated. The coordination compound formed between I and Hg^{2+} was found to be 2 : 1 in stoichiometry, which was confirmed from the Job's plot by UV-VIS spectrometry. The strong interaction of receptor I with the Hg^{2+} ions was supported by FT-IR measurements. The receptor I–Hg^{2+} complex was centrifuged, washed with water, and dried in vacuum. The obvious infrared absorption peak at 1115 cm^{-1} was ascribed to the characteristic stretching vibration band of the group of Hg(II) perchlorate trihydrate ($Hg(ClO_4)_2 \cdot 3H_2O$) (Fig. S6. In addition, the FT-IR shows the existence of the CN absorption and the band shift of NH_2 (from 3323 cm^{-1} and 3385 cm^{-1} to 3379 cm^{-1} and 3468 cm^{-1}) and the weakening of the pyridinyl group. The result was also confirmed by MS analysis. The addition of 1 mM Hg^{2+} solution to a 2 mM solution of I in ethanol led to the formation of a precipitate. The precipitate was isolated by centrifugation and purified by repeated washings with ethanol. Mass spectral analysis of the precipitated product showed a mass ion peak at m/z 679.5115 (calc. 679.1745), corresponding to $[2I + Hg^{2+} + ClO_4^- + 2H_2O - HClO_4)]^+$, indicating a 2 : 1 adduct of I and Hg^{2+}. Moreover, the elemental analysis results of the metal complex showed N 10.05 %, C 41.14 %, H 2.81 % (calculated: N 9.46 %,

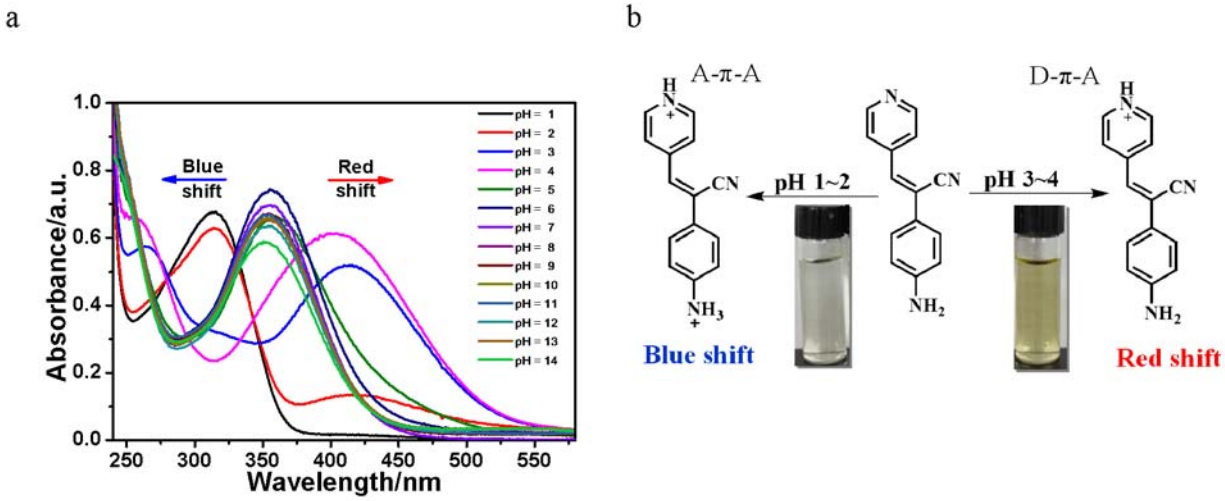

Fig. 10. Effect of pH on interaction of I in water (a); scheme of molecular level interactions involved (b).

Brought to you by | New York University Bobst Library Technical Services
Authenticated
Download Date | 5/27/15 5:46 PM

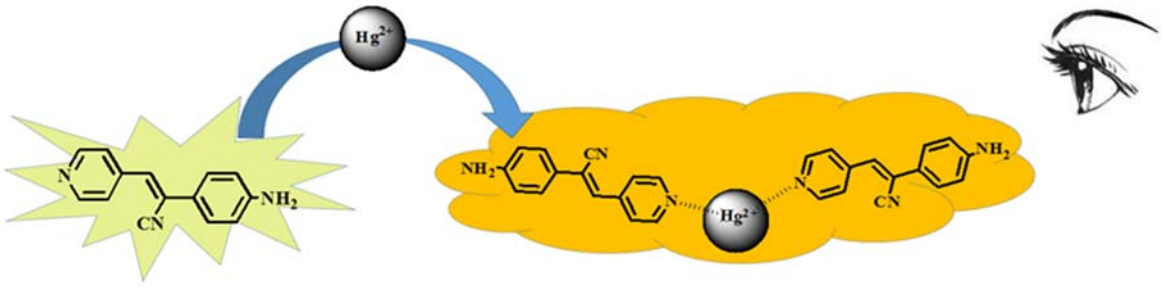

Fig. 12. Proposed binding mechanism of Hg^{2+} by *I*.

C 40.57 %, H 3.18 %), providing further evidence of a 2 : 1 complex formation. Additionally, ^{1}H NMR titration experiments were conducted to gain an insight into the essence of the coordination of Y1 by Hg^{2+}. The partial ^{1}H NMR spectra of both *I* and the *I*–Hg^{2+} adduct are shown in Fig. 11 (Xie et al., 2013). Upon the addition of 0.5 equiv. of Hg^{2+} ions to the solution of *I*, the chemical shift of the all proton (Fig. 11a) showed a downfield shift, as anticipated (Fig. 11b). Due to the decrease in electron density in the pyridine ring moiety, the protons on the pyridine ring moiety of *I* (H1 and H2 in Figs. 11a and 11b, respectively) exhibited a significant downfield shift, which suggested that the nitrogen atom of the pyridine ring moiety of *I* was participating in the complexation with Hg^{2+}. This coordination led to the changes in the absorption. Moreover, with increasing the concentration of Hg^{2+}, the maximal absorption wavelength of probe *I* exhibited a red shift from 490 nm to 570 nm in DMSO (Fig. S7). On the basis of the above experimental results, a plausible mode of binding *I* with Hg^{2+} in a ratio of 2 : 1 is proposed, as shown in Fig. 12.

Conclusions

A readily-prepared and simple structural colorimetric sensor *I* for Hg^{2+} was designed and synthesised. Comparison with *II* indicated that the strong donor group (NH_2) acted as a signal group and played an important role in the process of colorimetric recognition. Upon the reaction of *I* with Hg^{2+} in an aqueous ethanol solution, a distinct colour change from light yellow to orange occurred immediately, rendering the "naked-eye" detection of Hg^{2+} ions possible. Significantly, the obvious colour change exhibited a high selectivity and sensitivity to Hg^{2+} between the other common metal ions, forming a stable 2 : 1 *I*–Hg^{2+} complex. This work extends the range of possible methods to detect Hg^{2+} ions in biological, chemical and environmental samples.

Acknowledgements. This work was financially supported by the National Natural Science Foundation of China (nos. 21101001, 50873001 and 61107014), the Educational Commission of Anhui Province of China (no. KJ20142D02),the 211 Project of Anhui University, and the Team for Scientific Innovation Foundation of Anhui Province (no. 2006KJ007TD).

Supplementary data

The supplementary data associated with this article (A simple pyridine-based colorimetric chemosensor for highly sensitive and selective mercury(II) detection with the naked eye) can be found in the online version of this paper (DOI: 10.1515/chempap-2015-0061).

References

Aït-Haddou, H., Wiskur, S., Lynch, V., & Anslyn, E. V. (2001). Achieving large color changes in response to the presence of amino acids: A molecular sensing ensemble with selectivity for aspartate. *Journal of the American Chemical Society*, *123*, 11296–11297. DOI: 10.1021/ja011905v.

Azevedo-Pereira, H. M. V. S., & Soares, A. M. V. M. (2010). Effects of mercury on growth, emergence and behavior of *Chironomus riparius* Meigen (Diptera: Chironomidae). *Archives of Environmental Contamination and Toxicology*, *59*, 216–224. DOI: 10.1007/s00244-010-9482-9.

Bera, K., Das, A. K., Nag, M., & Basak, S. (2014). Development of a rhodamine–rhodanine-based fluorescent mercury sensor and its use to monitor real-time uptake and distribution of inorganic mercury in live zebrafish larvae. *Analytical Chemistry*, *86*, 2740–2746. DOI: 10.1021/ac404160v.

Carter, K. K., Rycenga, H. B., & McNeil, A. J. (2014). Improving Hg-triggered gelation via structural modifications. *Langmuir*, *30*, 3522–3527. DOI: 10.1021/la404567b.

Chemnasiri, W., & Hernandez, F. E. (2012). Gold nanorod-based mercury sensor using functionalized glass substrates. *Sensors and Actuators B: Chemical*, *173*, 322–328. DOI: 10.1016/j.snb.2012.07.002.

Chen, Q. Y., & Chen, C. F. (2005). A new Hg^{2+}-selective fluorescent sensor based on a dansyl amide-armed calix[4]-aza-crown. *Tetrahedron Letters*, *46*, 165–168. DOI: 10.1016/j.tetlet.2004.10.169.

Chen, H., Ji, X., Zhang, S., Shi, W., Wei, M., Evans, D. G., & Duan, X. (2013). A ratiometric fluorescence chemosenser for Hg^{2+} based on primuline and layered double hydroxide ultrafilms. *Sensors and Actuators B: Chemical*, *178*, 155–162. DOI: 10.1016/j.snb.2012.12.075.

Cheng, X. H., Li, Q. Q., Li, C. G., & Li, Z. (2011). Azobenzene-based colorimetric chemosensors for rapid naked-eye detection of mercury(II). *Chemistry – A European Journal*, *17*, 7276–7281. DOI: 10.1002/chem.201003275.

Coronado, E., Galán-Mascarós, J. R., Martí-Gastaldo, C., Palomares, E., Durrant, J. R., Vilar, R., Gratzel, M., & Nazeeruddin, M. K. (2005). Reversible colorimetric probes for mer-

Brought to you by | New York University Bobst Library Technical Services
Authenticated
Download Date | 5/27/15 5:46 PM

cury sensing. *Journal of the American Chemical Society*, *127*, 12351–12356. DOI: 10.1021/ja0517724.

Dalapati, S., Paul, B. K., Jana, S., & Guchhait, N. (2011). Highly selective and sensitive fluorescence reporter for toxic Hg(II) ion by a synthetic symmetrical azine derivative. *Sensors and Actuators B: Chemical*, *157*, 615–620. DOI: 10.1016/j.snb.2011.05.034.

Farhadi, K., Forough, M., Molaei, R., Hajizadeh, S., & Rafipour, A. (2012). Highly selective Hg^{2+} colorimetric sensor using green synthesized and unmodified silver nanoparticles. *Sensors and Actuators B: Chemical*, *161*, 880–885. DOI: 10.1016/j.snb.2011.11.052.

Goswami, S., Das, S., & Aich, K. (2013). An ICT based highly selective and sensitive sulfur-free sensor for naked eye as well as fluorogenic detection of Hg^{2+} in mixed aqueous media. *Tetrahedron Letters*, *54*, 4620–4623. DOI: 10.1016/j.tetlet.2013.06.035.

Gundacker, C., Gencik, M., & Hengstschläger, M. (2010). The relevance of the individual genetic background for the toxicokinetics of two significant neurodevelopmental toxicants: Mercury and lead. *Mutation Research/Reviews in Mutation Research*, *705*, 130–140. DOI: 10.1016/j.mrrev.2010.06.003.

Gunnlaugsson, T., Kruger, P. E., Jensen, P., Tierney, J., Ali, H. D. P., & Hussey, G. M. (2005). Colorimetric "naked eye" sensing of anions in aqueous solution. *The Journal of Organic Chemistry*, *70*, 10875–10878. DOI: 10.1021/jo0520487.

Guo, Z. Q., Zhu, W. H., Zhu, M. M., Wu, X. M., & Tian, H. (2010). Near-infrared cell-permeable Hg^{2+} -selective ratiometric fluorescent chemodosimeters and fast indicator paper for $MeHg^{+}$ based on tricarbocyanines. *Chemistry – A European Journal*, *16*, 14424–14432. DOI: 10.1002/chem.201001769.

Hansen, S., Nieboer, E., Sandanger, T. M., Wilsgaard, T., Thomassen, Y., Veyhe, A. S., & Odland, J. Ø. (2011). Changes in maternal blood concentrations of selected essential and toxic elements during and after pregnancy. *Journal of Environmental Monitoring*, *13*, 2143–2152. DOI: 10.1039/c1em10051c.

Hu, S. Z., & Chen, C. F. (2011). Hg^{2+} recognition by triptycene-derived heteracalixarenes: Selectivity tuned by bridging heteroatoms and macrocyclic cavity. *Organic & Biomolecular Chemistry*, *9*, 5838–5844. DOI: 10.1039/c1ob05515a.

Huang, J. H., Gao, X., Jia, J. J., Kim, J. K., & Li, Z. G. (2014). Graphene oxide-based amplified fluorescent biosensor for Hg^{2+} detection through hybridization chain reactions. *Analytical Chemistry*, *86*, 3209–3215. DOI: 10.1021/ac500192r.

Jenssen, M. T. S., Brantsæter, A. L., Haugen, M., Meltzer, H. M., Larssen, T., Kvalem, H. E., Birgisdottir, B. E., Thomassen, Y., Ellingsen, D., Alexander, J., & Knutsen, H. K. (2012). Dietary mercury exposure in a population with a wide range of fish consumption – self-capture of fish and regional differences are important determinants of mercury in blood. *Science of The Total Environment*, *439*, 220–229. DOI: 10.1016/j.scitotenv.2012.09.024.

Kim, H. J., Park, J. E., Choi, M. G., Ahn, S. D., & Chang, S. K. (2010). Selective chromogenic and fluorogenic signalling of Hg^{2+} ions using a fluorescein–coumarin conjugate. *Dyes and Pigments*, *84*, 54–58. DOI: 10.1016/j.dyepig.2009.06.009.

Kim, H. N., Ren, W. X., Kim, J. S., & Yoon, J. Y. (2012). Fluorescent and colorimetric sensors for detection of lead, cadmium and mercury ions. *Chemical Society Reviews*, *41*, 3210–3244. DOI: 10.1039/c1cs15245a.

Koenig, S., Solé, M., Fernández-Gómez, C., & Díez, S. (2013). New insights into mercury bioaccumulation in deep-sea organisms from the NW Mediterranean and their human health implications. *Science of The Total Environment*, *442*, 329–335. DOI: 10.1016/j.scitotenv.2012.10.036.

Lee, M. H., Cho, B. K., Yoon, J. Y., & Kim, J. S. (2007). Selectively chemodosimetric detection of Hg(II) in aqueous media. *Organic Letters*, *9*, 4515–4518. DOI: 10.1021/ol7020115.

Li, X. H., Wu, Y. Q., Liu, Y., Zou, X. M., Yao, L. M., Li, F. Y., & Feng, W. (2014). Cyclometallated ruthenium complex-modified upconversion nanophosphors for selective detection of Hg^{2+} ions in water. *Nanoscale*, *6*, 1020–1028. DOI: 10.1039/c3nr05195a.

Liang, Z. Q., Wang, C. X., Yang, J. X., Gao, H. W., Tian, Y. P., Tao, X. T., & Jiang, M. H. (2007). A highly selective colorimetric chemosensor for detecting the respective amounts of iron(II) and iron(III) ions in water. *New Journal of Chemistry*, *31*, 906–910. DOI: 10.1039/b701201m.

Lu, F. N., Yamamura, M., & Nabeshima, T. (2013). A highly selective and sensitive ratiometric chemodosimeter for Hg^{2+} ions based on an iridium(III) complex via thioacetal deprotection reaction. *Dalton Transactions*, *42*, 12093–12100. DOI: 10.1039/c3dt50807b.

Madhu, S., Sharma, D. K., Basu, S. K., Jadhav, S., Chowdhury, A., & Ravikanth, M. (2013). Sensing Hg(II) in vitro and in vivo using a benzimidazole substituted BODIPY. *Inorganic Chemistry*, *52*, 11136–11145. DOI: 10.1021/ic401365x.

Mei, Q. B., Wang, L. X., Tian, B., Yan, F., Zhang, B., Huang, W., & Tong, B. H. (2012). A highly selective and naked-eye sensor for Hg^{2+} based on quinazoline-4(3*H*)-thione. *New Journal of Chemistry*, *36*, 1879–1883. DOI: 10.1039/c2nj40400a.

Misra, A., & Shahid, M. (2010). Chromo and fluorogenic properties of some azo-phenol derivatives and recognition of Hg^{2+} ion in aqueous medium by enhanced fluorescence. *The Journal of Physical Chemistry C*, *114*, 16726–16739. DOI: 10.1021/jp1049974.

Ren, W., Zhu, C. Z., & Wang, E. K. (2012). Enhanced sensitivity of a direct SERS technique for Hg^{2+} detection based on the investigation of the interaction between silver nanoparticles and mercury ions. *Nanoscale*, *4*, 5902–5909. DOI: 10.1039/c2nr31410j.

Shafeekh, K. M., Rahim, M. K. A., Basheer, M. C., Suresh, C. H., & Das, S. (2013). Highly selective and sensitive colourimetric detection of Hg^{2+} ions by unsymmetrical squaraine dyes. *Dyes and Pigments*, *96*, 714–721. DOI: 10.1016/j.dyepig.2012.11.013.

Shellaiah, M., Wu, Y. H., Singh, A., Ramakrishnam Raju, M. V., & Lin, H. C. (2013). Novel pyrene- and anthracene-based Schiff base derivatives as Cu^{2+} and Fe^{3+} fluorescence turn-on sensors and for aggregation induced emissions. *Journal of Materials Chemistry A*, *1*, 1310–1318. DOI: 10.1039/c2ta00574c.

Sheng, R. L., Wang, P. F., Liu, W. M., Wu, X. H., & Wu, S. K. (2008). A new colorimetric chemosensor for Hg^{2+} based on coumarin azine derivative. *Sensors and Actuators B: Chemical*, *128*, 507–511. DOI: 10.1016/j.snb.2007.07.069.

Thirupathi, P., Saritha (née Gudelli), P., & Lee, K. H. (2014). Ratiometric fluorescence chemosensor based on tyrosine derivatives for monitoring mercury ions in aqueous solutions. *Organic & Biomolecular Chemistry*, *12*, 7100–7109. DOI: 10.1039/c4ob01044b.

Tian, M. Q., & Ihmels, H. (2011). Selective colorimetric detection of Hg^{2+} and Mg^{2+} with crown ether substituted *N*-aryl-9-aminobenzo[*b*]quinolizinium derivatives. *European Journal of Organic Chemistry*, *2011*, 4145–4153. DOI: 10.1002/ejoc.201100329.

Wang, K., Yang, L. X., Zhao, C., & Ma, H. M. (2013). 4-(8-Quinolyl)amino-7-nitro-2,1,3-benzoxadiazole as a newcolorimetric probe for rapid and visual detection of Hg^{2+}. *Spectrochimica Acta Part A*, *105*, 29–33. DOI: 10.1016/j.saa.2012.11.114.

Brought to you by | New York University Bobst Library Technical Services
Authenticated
Download Date | 5/27/15 5:46 PM

Wei, T. B., Li, J. J., Bai, C. B., Lin, Q., Yao, H., Xie, Y. Q., & Zhang, Y. M. (2013). A highly selective colorimetric sensor for Hg^{2+} based on a copper(II) complex of thiosemicarbazone in aqueous solutions. *Science China Chemistry*, *56*, 923–927. DOI: 10.1007/s11426-013-4863-3.

Wen, J. H., Geng, Z. R., Yin, Y. X., & Wang, Z. L. (2011). A versatile water soluble fluorescent probe for ratiometric sensing of Hg^{2+} and bovine serum albumin. *Dalton Transactions*, *40*, 9737–9745. DOI: 10.1039/c1dt10362h.

Wu, S. P., Du, K. J., & Sung, Y. M. (2010). Colorimetric sensing of Cu(II): Cu(II) induced deprotonation of an amide responsible for color changes. *Dalton Transactions*, *39*, 4363–4368. DOI: 10.1039/b925898a.

Xie, R. J., Yi, Y. R., He, Y., Liu, X. G., & Liu, Z. X. (2013). A simple BODIPY–imidazole-based probe for the colorimetric and fluorescent sensing of Cu(II) and Hg(II). *Tetrahedron*, *69*, 8541–8546. DOI: 10.1016/j.tet.2013.07.059.

Xing, X. Q., Du, R., Li, Y. F., Li, B., Cai, Q., Mo, G., Gong, Y., Chen, Z. G., & Wu, Z. H. (2013). Structural change of human hair induced by mercury exposure. *Environmental Science & Technology*, *47*, 11214–11220. DOI: 10.1021/es402335k.

Yang, M. H., Thirupathi, P., & Lee, K. H. (2011). Selective and sensitive ratiometric detection of Hg(II) ions using a simple amino acid based sensor. *Organic Letters*, *13*, 5028–5031. DOI: 10.1021/ol201683t.

Zhao, Q. H., Wang, Y., Cao, Y., Chen, A. G., Ren, M., Ge, Y. S., Yu, Z. F., Wan, S. Y., Hu, A. L., Bo, Q. L., Ruan, L., Chen, H., Qin, S. Y., Chen, W. J., Hu, C. L., Tao, F. B., Xu, D. X., Xu, J., Wen, L. P., & Li, L. (2014). Potential health risks of heavy metals in cultivated topsoil and grain, including correlations with human primary liver, lung and gastric cancer, in Anhui province, Eastern China. *Science of The Total Environment*, *470–471*, 340–347. DOI: 10.1016/j.scitotenv.2013.09.086.

Zhong, K. L., Zhou, X., Hou, R. B., Zhou, P., Hou, S. H., Bian, Y. J., Zhang, G., Tang, L. J., & Shang, X. H. (2014). A water-soluble highly sensitive and selective fluorescent sensor for Hg^{2+} based on 2-(2-(8-hydroxyquinolin)-yl)benzimidazole via ligand-to-metal charge transfer (LMCT). *RSC Advances*, *4*, 16612–16617. DOI: 10.1039/c4ra00060a.

Zhou, H. P., Wang, J. Q., & Chen, Y. X., Xi, W. G., Zheng, Z., Xu, D. L., Cao, Y. L., Liu, G., Zhu, W. J., Wu, J. Y., & Tian, Y. P. (2013). New diaminomaleonitrile derivatives containing aza-crown ether: Selective, sensitive and colorimetric chemosensors for Cu(II). *Dyes and Pigments*, *98*, 1–10. DOI: 10.1016/j.dyepig.2013.01.018.

Zhu, M., Yuan, M. J., Liu, X. F., Xu, J. L., Lv, J., Huang, C. S., Liu, H. B., Li, Y. L., Wang, S., & Zhu, D. B. (2008). Visible near-infrared chemosensor for mercury ion. *Organic Letters*, *10*, 1481–1484. DOI: 10.1021/ol800197t.

Brought to you by | New York University Bobst Library Technical Services
Authenticated
Download Date | 5/27/15 5:46 PM